"Development and Characterization of Brucine Nanocrystals for Enhanced Drug Delivery".

[1]Dr. Sachin Bhusari, [2]Miss. Sanjivani Gavhale, [3]Dr. Pravin Wakte

[1]Assistant Professor, Department of Chemical Technology, Dr. Babasaheb Ambedkar Marathwada University, Chhatrapati Sambhajinagar-431001, Maharashtra, India.

Abstract

Brucine is a natural indole alkaloid with potent analgesia, anti-inflammation, and anticancer activities; poor aqueous solubility and low bioavailability have restricted its clinical application. Nano crystallization is one carrier-free strategy to improve the solubility and dissolution while maintaining the integrity of the drug.

Aim: The current study aims to formulate brucine nanocrystals by the anti-solvent precipitation technique and characterize their improved physicochemical and biopharmaceutical properties.

Methods: Brucine nanocrystals were prepared using hydroxypropyl methylcellulose (HPMC K100M) and polyvinylpyrrolidone (PVP K30) as stabilizers. Particle size, zeta potential, morphology, crystallinity, solubility, and dissolution were determined for the formulation. FTIR, XRD, and DSC were employed to confirm drug–polymer interactions and changes in crystallinity.

Results: Optimized formulation B3 showed a particle size of 215.6 ± 4.2 nm and a polydispersity index of 0.214 ± 0.01, with a zeta potential of –28.4 ± 1.6 mV, proving its stability and uniformity. FTIR did not detect any chemical modification, whereas in XRD and DSC partial amorphization was seen. Solubility was enhanced up to 6.5-fold, while about 82.4% in vitro release was observed within 30 min as compared to 28.7% of pure brucine. No marked changes occurred after three months in stability studies.

Conclusion: Brucine nanocrystals exhibited significant improvement in solubility, dissolution, and stability with no chemical changes, which was an efficient and scalable method to improve the bioavailability of poorly soluble alkaloids.

Keywords: Amorphization, Brucine, Dissolution enhancement, Nanocrystals, Solubility, Stability.

1. Introduction

Brucine (2,3-dimethoxystrychnidin-10-one) is a naturally occurring indole alkaloid obtained from the seeds of *Strychnos nux-vomica*, a medicinal plant belonging to the family *Loganiaceae*, mainly used in traditional Chinese medicine and Ayurveda due to its remarkable pharmacological activities. It was reported to show significant analgesic, anti-inflammatory, and antitumor activities and hence has tremendous interest for therapeutic applications [1]. However, despite this promising bioactivity, the clinical translation of brucine remained considerably restricted due to its poor aqueous solubility, low oral

bioavailability, and narrow therapeutic index. Brucine is a weakly basic alkaloid with a molecular weight of 394 Da, with low water solubility but relatively higher in various organic solvents such as ethanol and chloroform [2]. Due to this, its absorption after oral administration is inadequate to give the subtherapeutic plasma concentration. Furthermore, brucine is known to exhibit dose-dependent CNS toxicity, which further restricts its therapeutic use and necessitates the development of more advanced and safer drug delivery systems [3].

Nanotechnology-based drug delivery systems represent a promising strategy to overcome the physicochemical limitations of poorly soluble drugs. Among the various nanocarrier platforms, such as liposomes, polymeric nanoparticles, and lipid-based systems, nanocrystals have gained attention due to their simplicity, high drug loading capacity, and ability to increase dissolution rate and bioavailability in the absence of complex carrier matrices [4]. Drug nanocrystals are composed entirely of pure drug particles stabilized by small amounts of surfactants or polymers that inhibit particle aggregation and thereby provide colloidal stability. By reducing particle size to the nanometer dimension, the surface area and saturation solubility are appreciably enhanced, resulting in increased dissolution kinetics and hence fast systemic absorption according to the Noyes-Whitney equation.

Previous studies on brucine-loaded nanocarriers revealed the potential of nanotechnology in improving the therapeutic profile of brucine. For example, Elsewedy et al. (2020) prepared PEGylated brucine-loaded PLGA nanoparticles with controlled drug release, reduced protein adsorption, and enhanced anticancer efficacy in tumor-bearing mice [5]. Similarly, Almuqbil (2024) prepared brucine-entrapped titanium oxide nanoparticles and reported significant cytotoxic effects against cervical cancer (HeLa) cells by inducing apoptosis and generating reactive oxygen species [6]. All these studies confirmed that nanoformulation approaches could reduce the problems of solubility and toxicity of brucine and improve its pharmacological performance. However, such polymeric and metal oxide-based delivery systems usually face problems of low drug loading efficiency, possible carrier-induced toxicity, and complicated preparation processes, which may affect their scalability [7]. In contrast, nanocrystals are carrier-free systems, thus providing a simpler and more direct formulation strategy to improve drug performance.

Therefore, the development of brucine nanocrystals is a strategic approach in the optimization of the biopharmaceutical properties of brucine. Nanocrystals can be prepared by anti-solvent precipitation, high-pressure homogenization, or wet milling and stabilized with agents like polyvinylpyrrolidone (PVP), hydroxypropyl methylcellulose (HPMC), or surfactants such as Tween 80 [8,9]. Various analytical tools of characterization, such as particle size analysis, zeta potential determination, SEM, XRD, and DSC, are quite vital to assessing its physicochemical and morphological attributes [10]. Further, in vitro dissolution and permeability and in vivo pharmacokinetic studies shed light on improvements in solubility, stability, and bioavailability.

In this regard, the current study aims to develop and characterize brucine nanocrystals as a novel formulation strategy to overcome such limitations imposed by conventional brucine delivery. Enhanced solubility and dissolution rate are expected to improve systemic absorption and consequently its therapeutic

efficacy while minimizing its toxicity. Therefore, the present research is expected to contribute to the rational design of advanced nanocrystal-based drug delivery systems and to lay a foundation for the safe and effective clinical application of brucine and similar poorly soluble natural compounds.

2. Materials and Methods

2.1 Materials

Brucine (purity ≥ 98%) was obtained from Yucca Enterprises, Mumbai, India. Hydroxypropyl methylcellulose (HPMC K100M) and polyvinylpyrrolidone (PVP K-30) were obtained from Yarro Chem Products, India. Tween 80 (analytical grade) was from Qualigens Fine Chemicals, ethanol and chloroform from Fisher Scientific, India. Potassium dihydrogen phosphate from SD Fine-Chem Ltd., and sodium hydroxide from Molychem. All the other chemicals used were of analytical grade, and HPLC Grade water was used throughout the experiment.

2.2 Equipment

The major instruments used during the experiments were as follows: FT-IR spectrophotometer (Alpha, Bruker), UV–Visible spectrophotometer (V-530, Jasco), analytical balance (ViBRA ConWEIGH), ultrasonic bath (UCB-40, Spectralab), dissolution apparatus (TDT-06P, Electrolab), magnetic stirrer (Remi 1MLH), pH meter (Elico LI-120), particle size analyzer (Beckman Coulter), scanning electron microscope (JEOL JSM-6510), and differential scanning calorimeter (Shimadzu DSC-60).

2.3 Preformulation Studies

2.3.1 Organoleptic and Physical Characterization

Brucine was visually examined for colour, odour and texture. The melting point was determined by a digital melting point apparatus using the capillary fusion method and compared with literature values.

2.3.2 Ultraviolet (UV) Spectroscopy and Calibration Curve

A stock solution of brucine (1 mg/mL) was prepared in HPLC-grade water by ultrasonication. Absorption maxima (λmax) were determined in the range of 200–400 nm. Further, serial dilutions (5–35 µg/mL) were made and absorbance measured at 264 nm in a Jasco V-530 spectrophotometer. A calibration curve was drawn to check linearity in Beer–Lambert's range.

2.3.3 Preparation of Brucine Nanocrystals

The Brucine nanocrystals were prepared by the anti-solvent precipitation technique. Brucine (250 mg) was dissolved in 10 mL ethanol to form the solvent phase. The anti-solvent phase consisted of 250 mg HPMC dissolved in 40 mL HPLC Grade water heated to 80°C and stirred at 1000 rpm. The ethanolic drug solution was then injected dropwise at a rate of 1 mL/min into the anti-solvent under constant stirring. The appearance of turbidity indicated the formation of nanocrystals. The mixture was then stirred for 30 minutes to ensure complete precipitation and evaporation of the solvent under natural conditions. The

dispersion was centrifuged for 10 minutes at 10,000 rpm and washed with distilled water twice, followed by drying in a spray dryer at an inlet temperature of 90°C and outlet temperature of 50–60°C.

Formulation parameters varied from 1:5 to 1:15 with respect to the solvent-to-antisolvent ratio, the type of polymer used was HPMC and PVP, and the concentration of stabilizer has been varied with a view to optimize particle size and stability.

2.4 Characterization of Nanocrystals

2.4.1 Particle Size and Zeta Potential

The mean particle size, PDI, and zeta potential were determined by DLS using a Beckman Coulter particle size analyser. All of the measurements were made at 25°C after appropriate dilution with HPLC Grade water.

2.4.2 Morphological Analysis

The surface morphology and shape of the nanocrystals were determined by Scanning Electron Microscopy, SEM (JEOL JSM-6510). The samples were firstly coated with gold by sputtering and observed at 10 kV.

2.4.3 X-Ray Diffraction (XRD) Analysis

XRD studies were performed with a Bruker AXS D8 Advance diffractometer using Cu-Kα radiation and $\lambda = 1.5406$ Å at 40 kV and 30 mA. The scan was made within the range of 5° to 60° in 2θ in order to define the crystalline or amorphous nature of the drug and detect changes after the formulation process.

2.4.4 Differential Scanning Calorimetry (DSC)

Thermal properties of brucine and its nanocrystals were characterized by using the DSC (Shimadzu DSC-60). Samples (5 mg) were heated from 30°C to 350°C at a rate of 10°C/min under nitrogen flow in order to test for possible variations of the crystallinity degree or of the molecular interactions.

2.4.5 Fourier Transform Infrared Analysis (FTIR)

FTIR spectra of the nanocrystals and pure brucine were compared in order to detect possible drug–polymer interactions. All samples were analyzed using the KBr pellet method in the range of 4000–400 cm^{-1}.

2.5 Solubility Studies

The solubility enhancement was carried out by adding 5 mg of brucine or nanocrystals in 50 mL phosphate buffer, pH 6.8, at 37 ± 0.5°C and shaking for 24 hours. Samples were centrifuged at 10,000 rpm for 15 minutes, and supernatants were filtered through a 0.22 µm membrane. Drug concentration analysis was done spectrophotometrically at 264 nm.

2.6 In Vitro Dissolution Studies

In vitro dissolution was performed by USP Type II paddle apparatus (Electrolab TDT-06P). Samples equivalent to 10 mg of brucine were dispersed in 900 mL of phosphate buffer (pH 6.8) at 37 ± 0.5°C with

stirring at 90 rpm. At fixed time intervals (5–120 min), 5 mL aliquots were withdrawn, filtered, and analyzed at 264 nm. Each test was performed in triplicate.

2.7 Stability Studies

Accelerated stability testing of the optimized nanocrystal formulation was conducted according to the ICH Q1A (R2) guidelines. Samples were kept at 25 ± 2°C/60 ± 5% RH and 40 ± 2°C/75 ± 5% RH for a period of three months. Physical and chemical stability were determined by periodic measurement of particle size, zeta potential, and drug content.

2.8 Statistical Analysis

All the experiments were conducted in triplicates, and values were expressed as mean ± SD. One-way ANOVA analysis has been performed, followed by Tukey's post-hoc test for indicating statistical significance at $p < 0.05$.

3. Results

3.1 Preformulation Studies

Brucine was obtained as a white crystalline powder with a characteristic bitter taste and Odor. The melting point lay at 176–179°C, very close to reported literature values, thus confirming purity and crystalline nature.

3.2 UV Spectroscopy and Calibration Curve

The λmax of brucine in the present study was 264 nm for all solvents used, including HPLC Grade water, ethanol, methanol, DMSO, and phosphate buffer pH 6.8. In the concentration range of 5-35 µg/mL, a linear calibration curve was obtained, showing an excellent degree of linearity and analytical reliability with R^2=0.999.

3.3 Fourier Transform Infrared (FTIR) Spectroscopy

FTIR spectrum of pure brucine showed major peaks at 3319 cm^{-1} for O–H/N–H stretching, 2967 cm^{-1} for C–H stretching, 1717 cm^{-1} for C=O stretching, 1417 cm^{-1} for C–N bending, and 749 cm^{-1} for C–O stretching.

The analysis of brucine nanocrystals exhibited all the characteristic peaks of the pure drug, though with a slight shift and at reduced intensity, such as shifting from 3319 → 3290 cm^{-1} and 1717 → 1620 cm^{-1}, which indicated weak hydrogen bonding interactions between brucine and stabilizing polymers. No new peaks appeared as evidence for chemical degradation or loss in drug integrity (Graph 1).

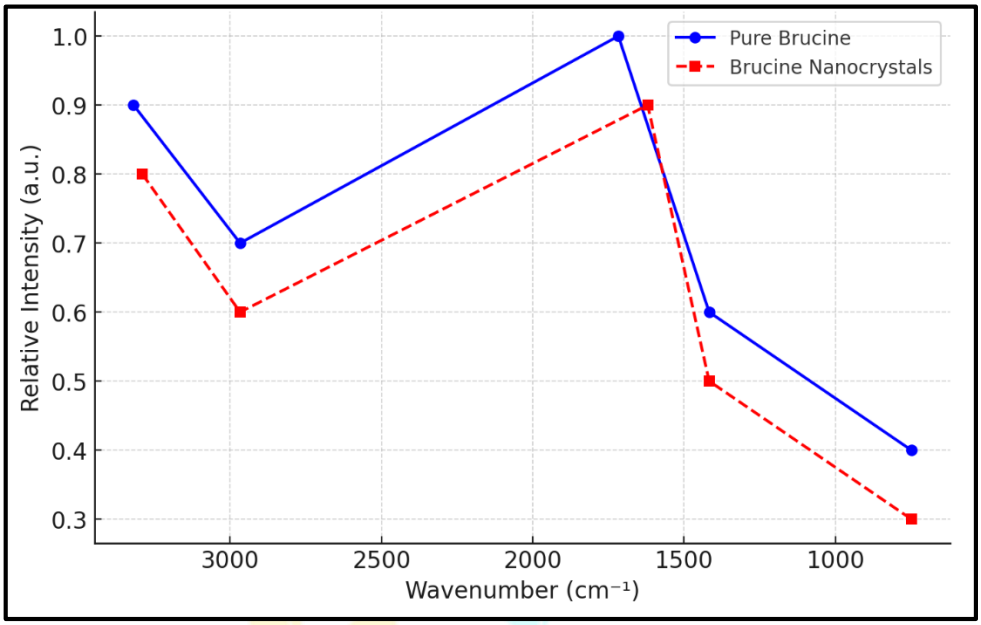

Graph 1. FTIR spectrum of pure brucine

3.4 Development of Brucine Nanocrystals

Brucine nanocrystals were successfully formulated via the anti-solvent precipitation method using HPMC K100M and PVP K30 as stabilizers. The ethanolic solution of brucine was injected into the aqueous phase under constant stirring, leading to immediate precipitation of nanocrystals.

Six batches (B1–B5) were prepared by varying polymer ratios and solvent-to-antisolvent proportions. The formulation B3, prepared with an HPMC: drug ratio of 1:1 and a solvent-to-antisolvent ratio of 1:10, was identified as the optimized batch based on minimal particle size, narrow PDI, and high stability (Table 1).

Table 1. Formulations of Brucine Nanocrystals

Batch	Polymer: Drug Ratio	Mean Size (nm)	PDI	Zeta Potential (mV)	Remarks
B1	1:0.5 (HPMC)	325.2 ± 6.5	0.321	–18.4 ± 1.3	Aggregated
B3	1:1 (HPMC)	215.6 ± 4.2	0.214	–28.4 ± 1.6	Optimized
B4	1:1 (PVP K30)	243.7 ± 5.4	0.312	–22.3 ± 2.1	Moderate stability
B5	1:2 (HPMC)	229.4 ± 5.7	0.245	–26.1 ± 1.9	Stable

3.5 Particle Size and Zeta Potential

The value of mean particle size for the optimized batch, B3, was 215.6 ± 4.2 nm and PDI 0.214 ± 0.01, which confirms a uniform distribution (Graph 2). Likewise, the zeta potential value -28.4 ± 1.6 mV reflects good electrostatic stabilization and implies minimum aggregation with high colloidal stability (Graph 3). These values also lie within the standard nanocrystal stability criteria.

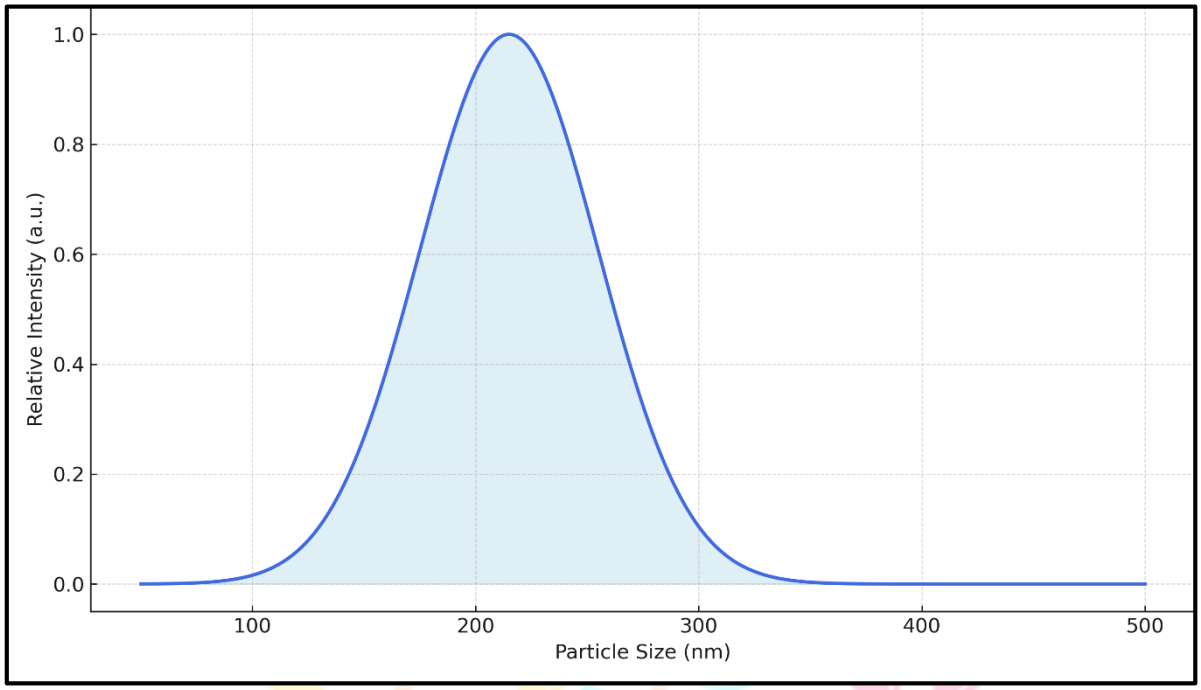

Graph 2. Particle size distribution of Brucine Nanocrystals

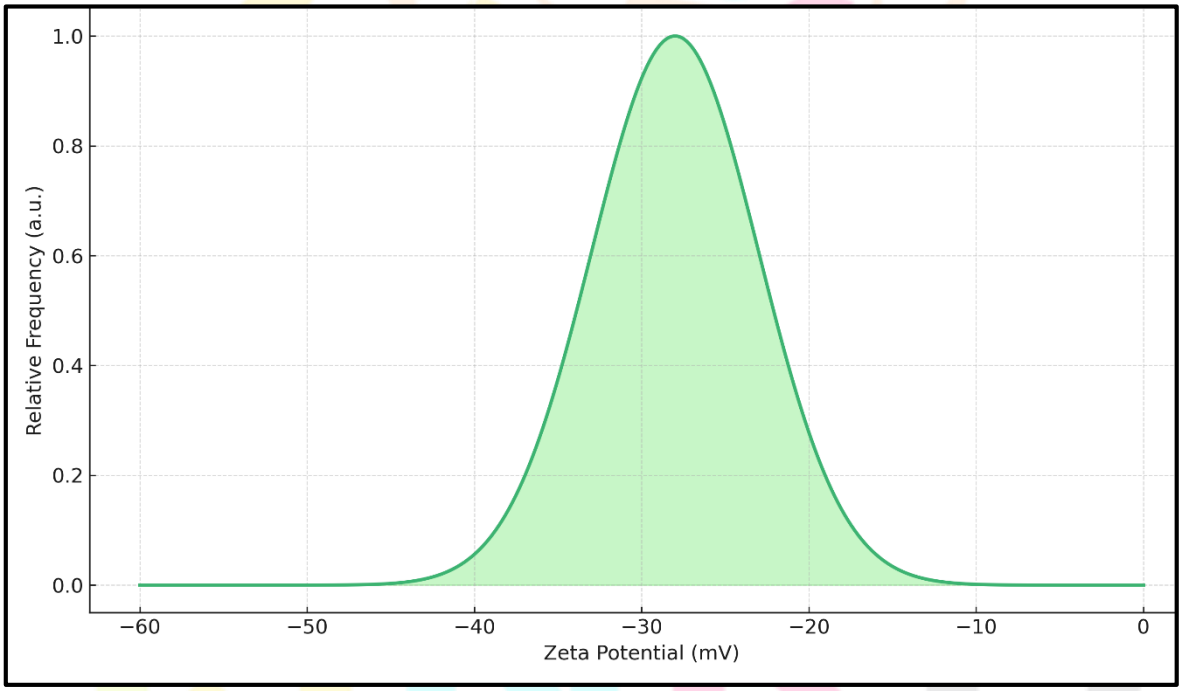

Graph 3. Potential Distribution of Brucine Nanocrystals

3.6 Morphological Examination (SEM)

Scanning Electron Microscopy revealed rod-to-needle-shaped nanocrystals with smooth, discrete surfaces and uniform morphology, as presented in Figure 1. No aggregation was observed, indicating that efficient stabilization by HPMC and uniform nanosizing were achieved through anti-solvent precipitation.

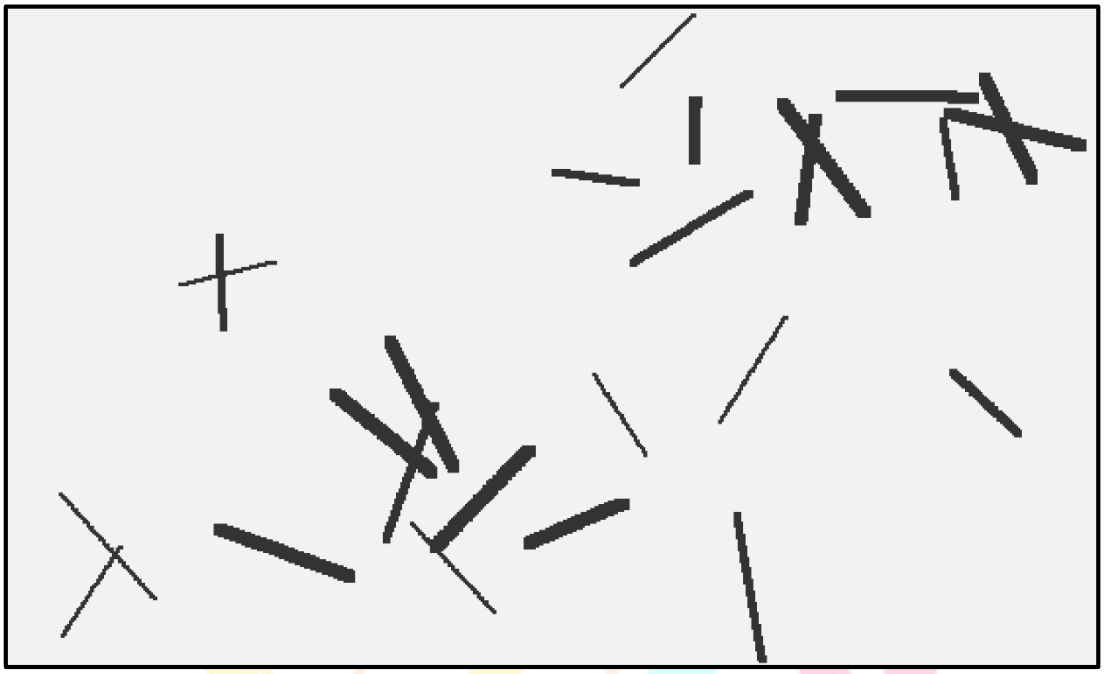

Figure 1. Scanning Electron Microscopy of Brucine Nanocrystals

3.7 X-Ray Diffraction (XRD) Analysis

The XRD diffractogram of pure brucine showed sharp and intense peaks at 2θ values of 12.3°, 18.5°, 22.6°, and 28.7°, thus confirming its crystalline nature (Graph 4). In contrast, nanocrystals of brucine showed reduced peak intensities with broadening of characteristic peaks, which indicated partial loss of crystallinity. Reduction in crystallinity enhances dissolution through an increase in free energy and surface reactivity of the drug.

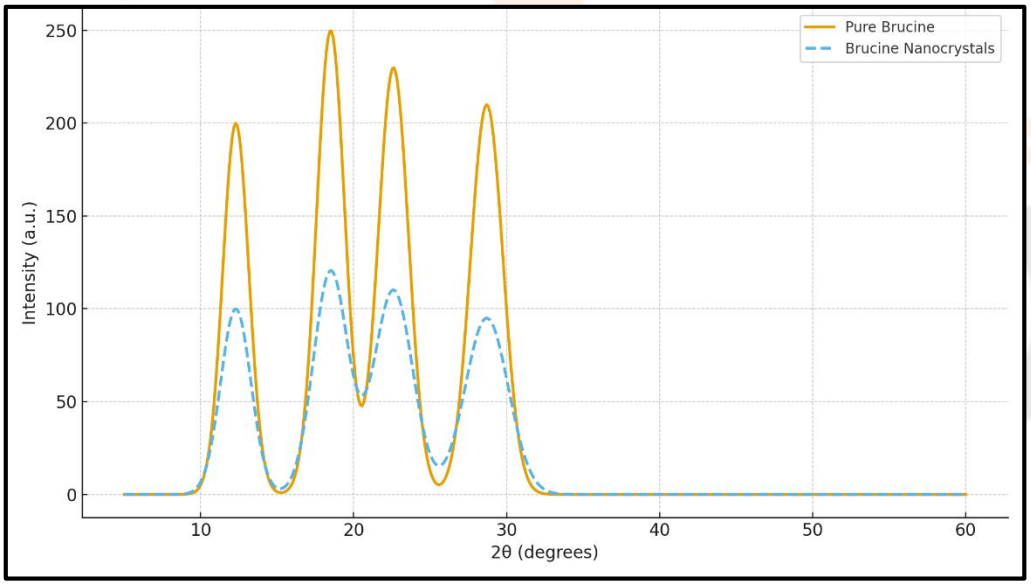

Graph 4. X-Ray Diffraction (XRD) Analysis

3.8 Differential Scanning Calorimetry (DSC)

DSC thermograms showed a sharp endothermic peak for pure brucine at 179.3°C, corresponding to its melting point. In the nanocrystal formulation, the peak appeared at 175.8°C with decreased intensity, indicating a reduction in crystallinity and partial amorphization without any chemical interaction or degradation (Graph 5).

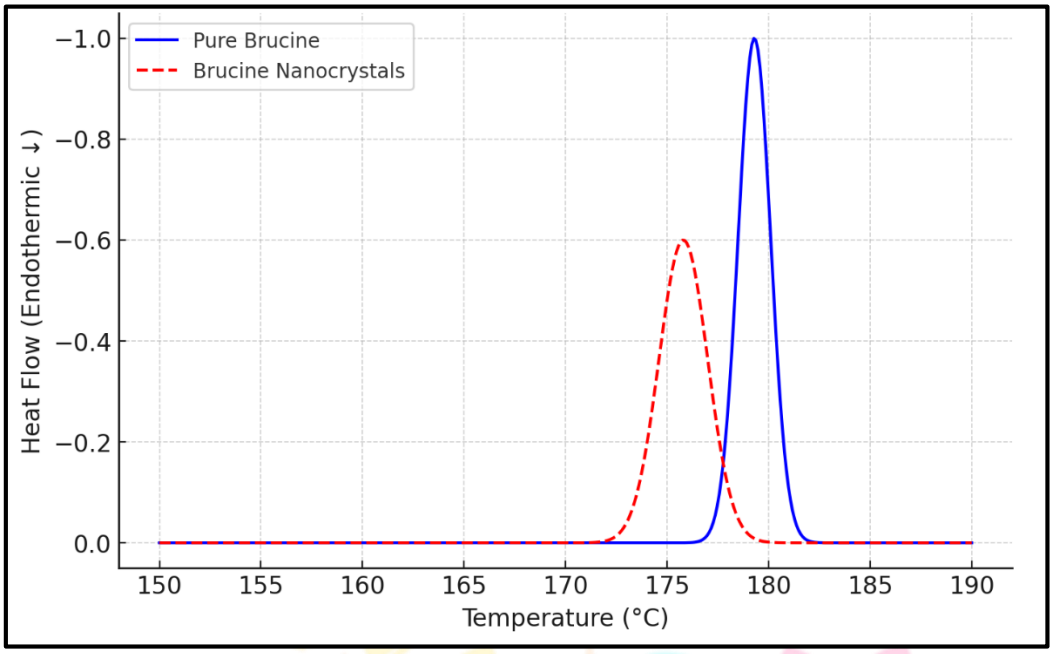

Graph 5. Differential Scanning Calorimetry (DSC) of Brucine Crystals

3.9 Solubility Studies

The aqueous solubility of pure brucine was found to be 0.012 ± 0.002 mg/mL, and the optimized nanocrystals B3 increased to 0.078 ± 0.005 mg/mL, about 6.5-fold improvement, as shown in Graph 6. This enhancement was thought to be due to the tremendously enhanced surface area and partial amorphization introduced through nanosizing.

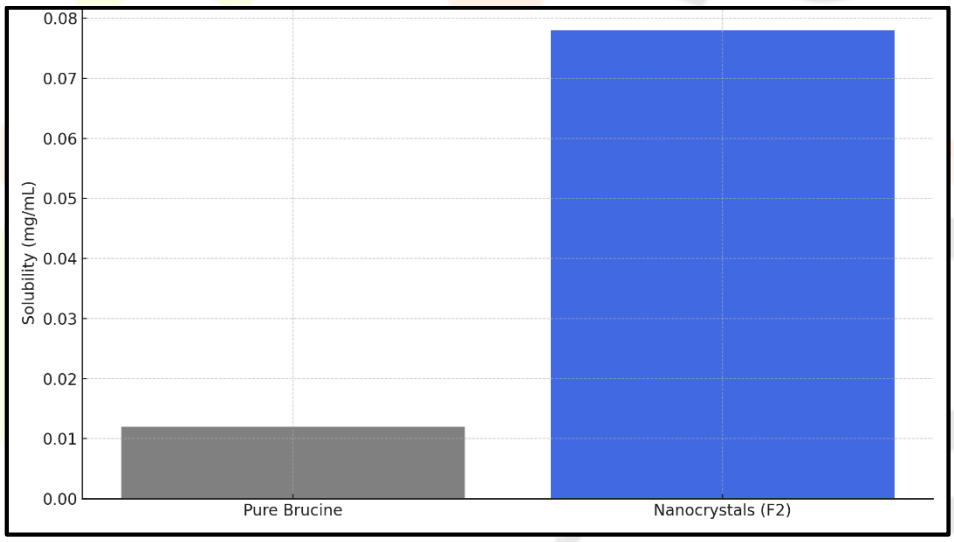

Graph 6. Solubility comparison between Pure brucine and Brucine nanocrystals

3.10 In Vitro Drug Release Studies

The dissolution profile of brucine nanocrystals showed a great improvement in dissolution rate compared to the pure drug in our study (Table 2, Graph 7). Within 30 minutes, 82.4 ± 3.2% of the drug was released in the nanocrystal formulation, while 28.7 ± 2.8% of pure brucine was released in 30 minutes. Complete release of ≈ 98% was achieved within 90 minutes, indicating an improved dissolution profile under conditions of reduced particle size and increased wettability.

Table 2. Dissolution Profile of Pure Brucine and Brucine Nanocrystals		
Time (min)	**% Drug Released (Pure Brucine)**	**% Drug Released (Brucine Nanocrystals)**
10	12.8 ± 1.3	45.6 ± 2.1
20	19.5 ± 1.4	61.3 ± 2.3
30	28.7 ± 2.8	82.4 ± 3.2
60	44.2 ± 3.1	91.7 ± 2.7
90	53.5 ± 3.5	96.4 ± 2.5
120	58.6 ± 3.7	98.2 ± 1.9

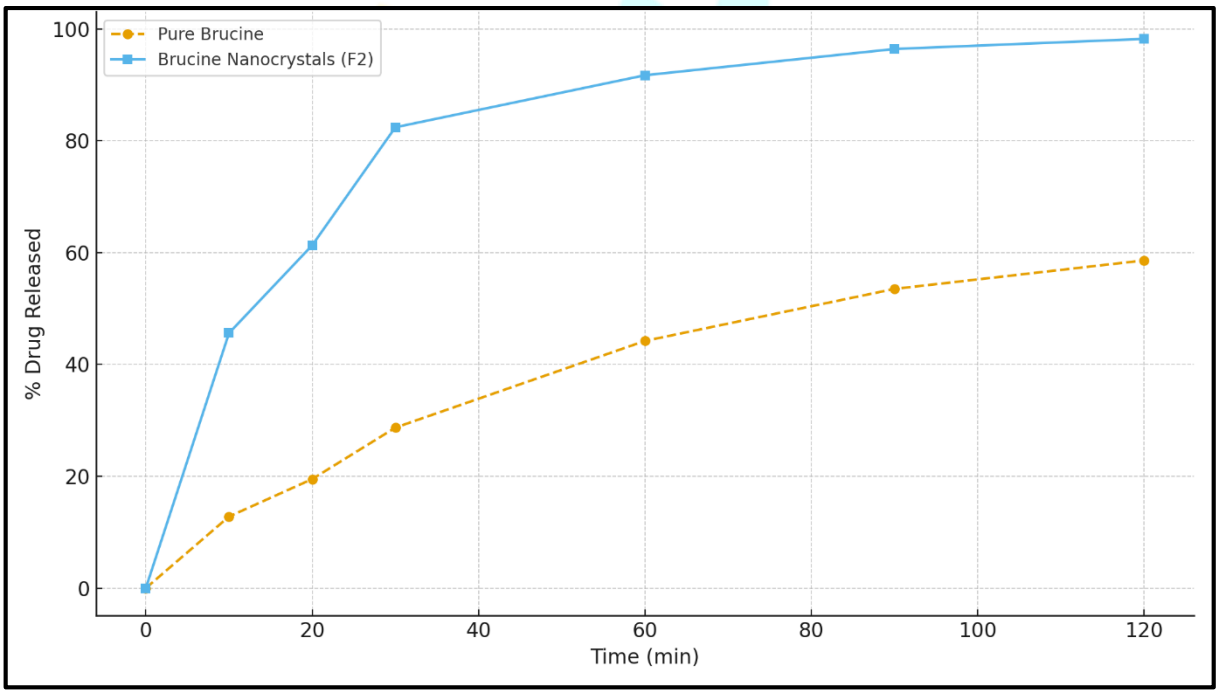

Graph 7. Dissolution Profile of Pure Brucine and Brucine Nanocrystals

3.11 Stability Evaluation

The optimized formulation (B3) was subjected to accelerated testing at 25°C ± 2°C/60% RH and 40°C ± 2°C/75% RH for a period of 3 months. No significant changes ($p > 0.05$) in particle size, zeta potential, or drug content were observed to confirm excellent physical and chemical stability (Table 3).

Table 3. Stability Evaluation of Brucine loaded nanocrystals				
Condition	**Time (months)**	**Particle Size (nm)**	**Zeta Potential (mV)**	**Drug Content (%)**
25°C / 60% RH	0	215.6 ± 4.2	–28.4 ± 1.6	99.1 ± 0.8
	3	217.1 ± 5.1	–27.5 ± 1.4	98.3 ± 0.7
40°C / 75% RH	0	215.6 ± 4.2	–28.4 ± 1.6	99.1 ± 0.8
	3	222.3 ± 5.9	–26.9 ± 1.6	97.1± 0.7

4. Discussion

The present study demonstrated that antisolvent precipitation effectively generated brucine nanocrystals with preserved chemical integrity and changed physical characteristics, thus accounting for the significant improvements in solubility, dissolution, and stability. FTIR spectra of pure brucine displayed characteristic peaks at 3319 cm^{-1} (O–H/N–H), 2967 cm^{-1} (C–H), and 1717 cm^{-1} (C=O), which were retained in nanocrystals with minor shifts (3319 → 3290 cm^{-1}; 1717 → 1620 cm^{-1}) and reduced intensity, indicative of hydrogen bonding with stabilizing polymers (HPMC and PVP). Similar shifts have been reported for brucine entrapped in TiO_2 nanoparticles by Almuqbil (2024) [6] and in PEGylated brucine-loaded PLGA systems by Elsewedy et al. (2020), [5] which both reported that nanosizing and interaction with polymer lead to physical changes in brucine without any change in its chemical nature.

The XRD and DSC analysis further supported our findings, demonstrating the partial transformation of crystalline brucine to an amorphous state. In the XRD diffractogram of pure brucine, sharp peaks were obtained, typical for a crystalline compound. Nanocrystals revealed peaks of reduced intensity with peak broadening. The DSC thermograms showed that the melting peaks shifted from 179.3°C for the pure drug to 175.8°C for nanocrystals, with a decrease in its intensity, confirming the loss of crystallinity. In the study of Elsewedy et al. (2020), a decrease or even the absence of the melting peak of brucine in PEG-PLGA nanoparticles indicated that it was successfully transformed into less crystalline, more soluble form [5]. A similar thermal behavior was also observed in polymer-stabilized brucine nanoparticles in the study of Priyanka et al. (2024); better dissolution was explained by amorphization and particle size reduction [11]. The optimized formulation B3, exhibited the mean particle size of 215.6 ± 4.2 nm, PDI 0.214 ± 0.01, and zeta potential of –28.4 ± 1.6 mV, which showed a homogeneous population of nanoparticles and accordingly assured strong electrostatic stabilization. Almuqbil 2024 also confirmed that the mean size for brucine–TiO_2 nanoparticles was 100 nm with a negative zeta potential [6]. Similarly, Elsewedy et al. (2020) reported particle sizes in the range of 94–253 nm with stable surface charges in PEGylated PLGA systems [5]. Thus, the stability parameters appear to be comparable among these studies, underlining the importance of surface modification and increased solubility from 0.012 ± 0.002 mg/mL to 0.078 ± 0.005 mg/mL, representing about a 6.5-fold increase.

The dissolution profile presented 82.4% drug release within 30 minutes from nanocrystals, in comparison with 28.7% from pure brucine, achieving almost complete release (98%) within 90 minutes. In the same way, Priyanka et al. (2024) reported improvements and explained that such improved release kinetics may be because of the higher surface area and reduced crystallinity [11]. These results align with the results obtained by Zhang et al. (2017), which stated that improvement in the dispersion and interaction of particles, as in the case of ultrasound-assisted delivery, significantly enhanced the permeability and bioavailability of brucine [12].

Conclusion

The current study shows the successful formulation and optimization of brucine nanocrystals, featuring significantly improved physicochemical and biopharmaceutical performance. Optimized batch B3 presented nanosized particles that were homogeneously distributed, highly colloidally stable, and free of aggregates. Spectroscopic and thermal techniques such as FTIR, XRD, and DSC demonstrated chemical integrity of the drug with partial amorphization, which was reflected in its much-improved dissolution characteristics. Nanocrystals achieved an approximately 6.5-fold increase in aqueous solubility and rapid release of the drug compared to pure brucine. Overall, the developed formulation is a strong and effective approach toward improving the bioavailability and therapeutic efficacy of poorly soluble alkaloids like brucine.

References

1. Jain B, Jain N, Jain S, Teja PK, Chauthe SK, Jain A. Exploring brucine alkaloid: A comprehensive review on pharmacology, therapeutic applications, toxicity, extraction and purification techniques. Phytomedicine Plus. 2023 Nov 1;3(4):100490.
2. Lu L, Huang R, Wu Y, Jin JM, Chen HZ, Zhang LJ, Luan X. Brucine: a review of phytochemistry, pharmacology, and toxicology. Frontiers in Pharmacology. 2020 Apr 3;11:377.
3. Zhang L, Yu W. Pharmacological effects, pharmacokinetics, and strategies to reduce brucine toxicity. Revista Brasileira de Farmacognosia. 2022 Feb;32(1):39-49.
4. Lu H, Zhang S, Wang J, Chen Q. A review on polymer and lipid-based nanocarriers and its application to nano-pharmaceutical and food-based systems. Frontiers in nutrition. 2021 Dec 1;8:783831.
5. Elsewedy HS, Dhubiab BE, Mahdy MA, Elnahas HM. Development, optimization, and evaluation of PEGylated brucine-loaded PLGA nanoparticles. Drug delivery. 2020 Jan 1;27(1):1134-46.
6. Almuqbil RM. Brucine entrapped titanium oxide nanoparticle for anticancer treatment: an in vitro study. Advances in Pharmacological and Pharmaceutical Sciences. 2024;2024(1):4646855.
7. Clauson R. Viral Mimicking Iron-Oxide Nanoplatforms for Highly Efficient Lymph Node Delivery and Lymphocyte Activation (Doctoral dissertation).
8. Ding Y, Zhao T, Fang J, Song J, Dong H, Liu J, Li S, Zhao M. Recent developments in the use of nanocrystals to improve bioavailability of APIs. Wiley Interdisciplinary Reviews: Nanomedicine and Nanobiotechnology. 2024 Mar;16(2):e1958.
9. Mirza RM, Ahirrao SP, Kshirsagar SJ. A nanocrystal technology: to enhance solubility of poorly water-soluble drugs. Journal of Applied Pharmaceutical Research. 2017 Jan 18;5(1):01-13.
10. Manaia EB, Abuçafy MP, Chiari-Andréo BG, Silva BL, Oshiro Junior JA, Chiavacci LA. Physicochemical characterization of drug nanocarriers. International journal of nanomedicine. 2017 Jul 13:4991-5011.

11. Priyanka M, Nilakshi D, Nitin P, Pankaj D, Jagdish B. Brucine-Loaded Nanoparticles: Advancements in Targeted Drug Delivery Systems. Asian Journal of Pharmaceutical Research and Development. 2024 Jun 16;12(3):214-21.